

Correlation between thermoluminescence and optically stimulated luminescence of α -Al₂O₃:C,Mg

Neilo Marcos Trindade^{1,2}, Luiz Gustavo Jacobsohn², Elisabeth Mateus Yoshimura³.

¹ Department of Physics, Federal Institute of Education, Science and Technology of São Paulo, São Paulo, SP, Brazil.

² Department of Materials Science and Engineering, Clemson University, Clemson, SC, USA.

³ University of São Paulo - USP, Institute of Physics, São Paulo, SP, Brazil

ABSTRACT

The optically stimulated luminescence (OSL) and thermoluminescence (TL) signals of an $\text{Al}_2\text{O}_3:\text{C},\text{Mg}$ single crystal were investigated as a function of the heating temperature and illumination time before readout, respectively. The TL and OSL results were analyzed in complementary ways, including the area under the curve, whole range and partial integration, and peak intensity. A correlation between the continuous decay of the main TL peak intensity (at 185 °C at a heating rate of 1 °C/s) against blue light (470 nm) illumination times and the decay of the OSL signal for higher temperatures was found. Both these results showed that the emptying of the OSL active trap was closely related to the emptying of the trap related to the main TL peak, indicating a correlation of both phenomena.

Keywords: $\text{Al}_2\text{O}_3:\text{C},\text{Mg}$; OSL; thermoluminescence

25 **1. INTRODUCTION**

26 Thermoluminescence (TL) corresponds to the light emission upon heating of
27 insulating or semiconducting materials previously exposed to ionizing radiation, besides
28 incandescence (blackbody radiation) [1]. These materials find application in radiation
29 dosimetry, particularly in medical physics (radiotherapy, radiation diagnosis and nuclear
30 medicine) [2]. Optically stimulated luminescence (OSL) is similar to TL but in this case
31 luminescence is stimulated by the absorption of optical energy instead of thermal energy
32 [3]. In recent years, OSL has established itself in radiation dosimetry based on the
33 development of dosimeters $\text{Al}_2\text{O}_3:\text{C}$ and BeO [4], together with the search for new OSL
34 dosimetric materials [5-7]. In OSL, optical stimulation releases charge carriers from the
35 traps [3] and the material emits a light signal related to the absorbed irradiation dose [4].
36 In order for TL and OSL to occur, there must be at least one type of electronic trap that
37 captures charge carriers in a localized energy level within the band gap, and a
38 recombination center from where light is emitted.

39 $\text{Al}_2\text{O}_3:\text{C,Mg}$ is well-known as a fluorescent nuclear track detector (FNTD) that
40 was originally introduced for optical data storage by Akselrod *et al.* [8]. This material has
41 been successfully used in dosimetry of neutrons, protons and heavy charged particles [9,
42 10] with superior sensitivity and functionality when compared to other FNTD materials
43 [11]. This material is sensitive to charged particles within a broad linear energy transfer
44 (LET) range requiring little or no post-exposure chemical processing, and being reusable
45 [11]. An additional advantage of $\text{Al}_2\text{O}_3:\text{C,Mg}$ is that laser-induced fluorescence allows
46 for non-destructive fast readout using confocal scanning microscopy [9, 12]. This way,
47 images can be processed automatically with tracks appearing in the form of bright spots
48 on a dark background that can be counted with an image processing software [13, 14].

49 $\text{Al}_2\text{O}_3:\text{C,Mg}$ single crystals contain high concentrations of F and F^+ centers [8,
50 10]. In contrast to the predecessor $\text{Al}_2\text{O}_3:\text{C}$, whose F luminescence centers have a long
51 lifetime of ~ 35 ms, $\text{Al}_2\text{O}_3:\text{C,Mg}$ luminescence occurs due the presence of high
52 concentrations of F^+ centers with a considerably shorter lifetime < 7 ns. Such a short
53 lifetime enables its use as a radiation dosimeter in applications requiring fast
54 luminescence response like dose mapping and real-time optical fiber dosimetry [15, 16].
55 Also, $\text{Al}_2\text{O}_3:\text{C,Mg}$ crystals contain high concentrations of $\text{F}_2^{2+}(2\text{Mg})$ [14] that form
56 $\text{F}_2^+(2\text{Mg})$ due to an ionizing radiation induced radiochromic transformation [12, 17].
57 Since the transformation rate is proportional to the absorbed dose, this material ends up
58 storing the cumulative radiation dose that can be read at 750 nm [18].

59 $\text{Al}_2\text{O}_3:\text{C,Mg}$ has been investigated for TL and OSL applications [11, 19, 20]. The
60 TL glow curve of $\text{Al}_2\text{O}_3:\text{C,Mg}$ shows a main peak around 170 °C (1 °C/s), that is a result
61 of emissions at 325, 415, 520 and 750 nm likely corresponding to F^+ , F , $\text{F}_2^{2+}(2\text{Mg})$ and
62 of $\text{F}_2^+(2\text{Mg})$ centers, respectively [16, 21, 22]. Recently, the luminescence of these defects
63 and their role as recombination centers in the TL process was investigated as a function
64 of temperature, from room temperature (RT) up to 400 °C [21].

65 The goal of this work is to investigate the correlation between the OSL and TL
66 signals of $\text{Al}_2\text{O}_3:\text{C,Mg}$ through the following measurements: (i) the TL signal emitted
67 after partial readouts of the OSL signal, and (ii) the OSL signal remaining after partial TL
68 measurements.

69

70 2. MATERIALS AND METHODS

71 The sample investigated was an $\text{Al}_2\text{O}_3:\text{C,Mg}$ single crystal grown by the
72 Czochralski technique by Landauer, Inc., Crystal Growth Division, Stillwater, OK, USA.

73 The single crystal was cut into a 8 x 1.6 x 0.5 mm³ rectangular parallelepiped with one
74 polished side. The sample mass was 48 mg.

75 OSL and TL measurements were carried out using a commercial automated
76 TL/OSL reader made by Risø National Laboratory (model DA-20). TL glow curves were
77 obtained using a heating rate of 1 or 5 °C/s, from RT to 300 °C. OSL emission was
78 stimulated using blue light emitting diodes (470 nm, FWHM = 20 nm) delivering 80
79 mW/cm² at the sample position in CW mode. Each OSL measurement was carried out
80 during 60 s with 90% of the maximum LED power. The TL and OSL signals were
81 detected with a bialkali photomultiplier tube behind an UV-transmitting, visible-
82 absorbing glass filter (Hoya U-340, 7.5 mm thick) that blocked the stimulation light while
83 transmitting part of the OSL/TL signal, and a 5 mm dia. mask. Irradiation was performed
84 at room temperature using the built-in ⁹⁰Sr/⁹⁰Y beta source of the TL/ OSL reader (dose
85 rate of 10 mGy/s) with a total dose of 100 mGy (10 s total exposure). Two protocols were
86 used to investigate the TL-OSL correlation, as follows:

87 *Protocol A: partial OSL*

88 1. Heating up to 300 °C at 5 °C/s (to empty the traps), followed by cooling to
89 RT
90 2. Irradiation for 10 s (100 mGy) at RT
91 3. CW-OSL measurement during a time interval t_{stop}
92 4. TL up to 300 °C at 1 °C/s

93 Steps #1 to 4 were repeated with the illumination time (t_{stop}) in step #3
94 increasing from 1 to 60s, in 1 s steps. First of all, a measure without any
95 influence of illumination time (partial OSL) was performed.

96

97

98 *Protocol B: partial TL*

99 1. Heating up to 300 °C at 5 °C/s (to empty the traps), followed by cooling to

100 RT

101 2. Irradiation for 10 s (100 mGy) at RT

102 3. TL measurement at 1 °C/s until stop temperature T_{stop}

103 4. CW-OSL measurement at RT for 60 s

104 Steps #1 to 4 were repeated with T_{stop} varying from 125 to 225 °C, in 5 °C steps.

105 First of all, a measure without any influence of temperature (partial TL) was

106 performed.

107 The TL and OSL results were analyzed in complementary ways, including the area

108 under the curve (TL and OSL, whole range and partial integration), and maximum

109 intensity (TL main peak at 185 °C; OSL initial signal). Since all measurements were

110 carried out with the same sample, results were not normalized by the sample mass.

111

112 **3. RESULTS AND DISCUSSION**

113 Figure 1 shows the TL glow curves of $\text{Al}_2\text{O}_3:\text{C},\text{Mg}$ single crystal obtained with

114 different illumination times, according to protocol A. The glow curves were dominated

115 by emission near 185 °C (TL main peak), in addition to other low intensity peaks at lower

116 temperatures. Previous works showed that the shallow traps related to these peaks are due

117 to the presence of Mg in the lattice [16], and that the main peak followed a first order

118 kinetics TL mechanism with a trap activation energy of 1.36 eV and frequency factor in

119 the range of 10^{14} s^{-1} [15].

120 In this work, we noted that the position of the main peak and the TL intensity in
121 the 60-125 °C range were not affected by the illumination time, which possibly indicates
122 that the traps related to these peaks are not optically active. On the other hand, a
123 significant decrease in the intensity of the main peak even for short illumination times
124 was observed and assigned to optical bleaching due to the partial OSL readouts. The TL
125 behavior as a function of the illumination time was further investigated through the
126 analysis of the area of the TL glow curve from RT to 60 °C and of the main TL peak (125-
127 225 °C), together with the peak intensity value of the TL main peak at 185 °C (Fig. 2).
128 The intensity of the main peak decreased continuously for the whole illumination time
129 interval (from 1 to 60 s), while the intensity of the RT-60 °C TL signal increased initially
130 and only after about 3 s of illumination it started to decrease. Further, the time decay of
131 these two regions of the TL glow curves was different, with the main peak decreasing
132 with a faster rate. The signal of the main TL peak essentially vanished after about 30 s
133 while that of the RT-60 °C TL region was still measurable up to 60 s. In order to better
134 illustrate the different behavior of both regions of the TL glow curve, the partial areas
135 were normalized to the respective area of the glow curve obtained with no illumination,
136 as shown in Fig. 2c. As an example, it was noted that after an illumination time of 10 s
137 the area of the TL main peak was reduced to 17 % of the initial value while 72 % of the
138 area of the RT-60 °C TL signal remained. The increase of the intensity and slower decay
139 rate observed in the RT-60 °C TL signal was tentatively assigned to a photo-transference
140 of charge carriers from the deep traps to the shallower traps during illumination (at RT)
141 [23]. As reported by Kalita et al [24], this material presents TL peaks at temperatures
142 higher than the maximum temperature used in this work (300°C), and the charge carriers
143 trapped in the centers related to these peaks may be released by the stimulation light and

144 be retrapped in the shallower traps, contributing to the augment of the low temperature
145 part of the glow curve. At longer illumination times, the carriers trapped in the shallower
146 traps related to the TL peak depicted in the inset of Figure 1 are also released.

147 The thermal cleaning of the OSL signal following protocol B is presented in Fig. 3
148 for selected OSL curves (for visual clarity), where a decrease of the OSL intensity can be
149 seen for higher T_{stop} temperature values. These curves were analyzed in terms of their
150 maximum intensity value (*i.e.*, initial OSL signal value) and the total area under the curve,
151 as shown in Fig. 4 as a function of T_{stop} . The behavior of both quantities was similar, with
152 both exhibiting three distinct temperature regimes: the first, from RT to 150 °C range
153 where the OSL signal remained essentially constant, followed by an intermediate
154 temperature regime (from 150 to 200 °C) where there was a steep decrease in the OSL
155 signal, and a third regime (>200 °C) where the OSL signal slowly decayed to zero. The
156 constancy of the integrated and the maximum OSL signal with heating treatments up to
157 about 150 °C (Fig. 4) showed that the kinetics of the shallower traps (*i.e.*, TL signal from
158 RT up to ~125 °C) did not play a major role in the generation of the OSL signal. Supporting
159 that traps related to these TL peaks are probably not optically active at this stimulation
160 wavelength. On the other hand, the as T_{stop} temperature reaches the range corresponding
161 to the TL main peak (125 to 150 °C), a large decay of the OSL signal (integrated and
162 maximum values) is observed, corroborating the hypothesis that the traps related to the
163 main TL peak are also emptied by the blue stimulation light. Moreover, the absence of
164 TL signal above ~225 °C corresponded to the absence of OSL signal. These results
165 suggested the OSL signal to be exclusively related to the trap related to the main TL peak.

166 Finally, Fig. 5 presents the integrated OSL and TL signals as a function of the
167 illumination time. In terms of the TL signal, both the main peak intensity (integration

168 interval: 125-225 °C), and whole glow curve intensity are shown. As expected, the OSL
169 signal increased with illumination time, with a small trend to a higher values, while the
170 TL signal continuously decreased to zero. The behavior of TL and OSL signals was
171 complementary, suggesting that heat or light stimulation were releasing charge carriers
172 from the same traps. The photo transference from deep traps probably is the phenomenon
173 responsible for the observed small trend of OSL signal to higher values for longer
174 illumination times.

175

176 **4. CONCLUSIONS**

177 In this work, the correlation between the TL and OSL signals of an $\text{Al}_2\text{O}_3:\text{C},\text{Mg}$
178 single crystal was investigated. The decay of the main TL peak at 185 °C (at a heating
179 rate of 1 °C/s) with blue light (470 nm) illumination and the decay of the OSL signal with
180 thermal treatments show a correlation between both phenomena. These results showed
181 that the emptying of the OSL active trap was closely related to the emptying of the trap
182 related to the main TL peak. Moreover, while heating the irradiated sample up to 150 °C
183 did not affect the OSL signal significantly, heating at higher temperatures rapidly
184 exhausted OSL emission.

185

186 **5. ACKNOWLEDGMENTS**

187 Funding for this work was provided by the Brazilian agency São Paulo Research
188 Foundation (FAPESP), Grant No. 2017/11663-1. E. M. Yoshimura thanks the CNPq
189 grant. This material is based upon work supported by the National Science Foundation
190 under Grant No. 1653016. The authors are grateful to Dr. M.S. Akselrod with Landauer,
191 Inc., Crystal Growth Division, Stillwater, OK, for the $\alpha\text{-Al}_2\text{O}_3:\text{C},\text{Mg}$ crystal.

6. REFERENCES

194 [1] S.W.S. McKeever, Thermoluminescence of Solids, Cambridge University Press,
195 Cambridge, 1985.

196 [2] J. Azorin Nieto, Present status and future trends in the development of
197 thermoluminescent materials, *Applied Radiation and Isotopes*, 117 (2016) 135-142.

198 [3] E.G. Yukihara, S.W.S. McKeever, *Optically Stimulated Luminescence: Fundamentals*
199 and Applications, UK: John Wiley and Sons, West Sussex, 2011.

200 [4] A.S. Pradhan, J.I. Lee, J.L. Kim, Recent developments of optically stimulated
201 luminescence materials and techniques for radiation dosimetry and clinical applications,
202 *Journal of Medical Physics / Association of Medical Physicists of India*, 33 (2008) 85-
203 99.

204 [5] E.G. Yukihara, E.D. Milliken, L.C. Oliveira, V.R. Orante-Barrón, L.G. Jacobsohn,
205 M.W. Blair, Systematic development of new thermoluminescence and optically
206 stimulated luminescence materials, *Journal of Luminescence*, 133 (2013) 203-210.

207 [6] J.R. Hazelton, E.G. Yukihara, L.G. Jacobsohn, M.W. Blair, R. Muenchhausen,
208 Feasibility of using oxyorthosilicates as optically stimulated luminescence detectors,
209 *Radiation Measurements*, 45 (2010) 681-683.

210 [7] M.W. Blair, L.G. Jacobsohn, S.C. Tornaga, O. Ugurlu, B.L. Bennett, E.G. Yukihara,
211 R.E. Muenchhausen, Nanophosphor aluminum oxide: Luminescence response of a
212 potential dosimetric material, *Journal of Luminescence*, 130 (2010) 825-831.

213 [8] M.S. Akselrod, A.E. Akselrod, S.S. Orlov, S. Sanyal, T.H. Underwood, New
214 aluminum oxide single crystals for volumetric optical data storage, in: *Optical Data*
215 *Storage*, Optical Society of America, Vancouver, 2003, pp. TuC3.

216 [9] M.S. Akselrod, G.J. Sykora, Fluorescent nuclear track detector technology – A new
217 way to do passive solid state dosimetry, *Radiation Measurements*, 46 (2011) 1671-1679.

218 [10] S.A. Eller, M.F. Ahmed, J.A. Bartz, M.S. Akselrod, G. Denis, E.G. Yukihara,
219 Radiophotoluminescence properties of Al₂O₃:C,Mg crystals, *Radiation Measurements*,
220 56 (2013) 179-182.

221 [11] M.S. Akselrod, Fundamentals of Materials, Techniques, and Instrumentation for
222 OSL and FNTD Dosimetry, *AIP Conference Proceedings*, 1345 (2011) 274-302.

223 [12] G. Klimpki, J.M. Osinga, R. Herrmann, M.S. Akselrod, O. Jäkel, S. Greilich, Ion
224 range measurements using fluorescent nuclear track detectors, *Radiation Measurements*,
225 56 (2013) 342-346.

226 [13] G.J. Sykora, M.S. Akselrod, F. Vanhavere, Performance of fluorescence nuclear
227 track detectors in mono-energetic and broad spectrum neutron fields, *Radiation*
228 *Measurements*, 44 (2009) 988-991.

229 [14] G.J. Sykora, M. Salasky, M.S. Akselrod, Properties of novel fluorescent nuclear
230 track detectors for use in passive neutron dosimetry, *Radiation Measurements*, 43 (2008)
231 1017-1023.

232 [15] J.M. Kalita, M.L. Chithambo, Thermoluminescence of α -Al₂O₃:C,Mg: Kinetic
233 analysis of the main glow peak, *Journal of Luminescence*, 182 (2017) 177-182.

234 [16] M.G. Rodriguez, G. Denis, M.S. Akselrod, T.H. Underwood, E.G. Yukihara,
235 Thermoluminescence, optically stimulated luminescence and radioluminescence
236 properties of Al₂O₃:C,Mg, *Radiation Measurements*, 46 (2011) 1469-1473.

237 [17] G.M. Akselrod, M.S. Akselrod, E.R. Benton, N. Yasuda, A novel Al₂O₃ fluorescent
238 nuclear track detector for heavy charged particles and neutrons, Nuclear Instruments and
239 Methods in Physics Research Section B: Beam Interactions with Materials and Atoms,
240 247 (2006) 295-306.

241 [18] M.F. Ahmed, S.A. Eller, J.A. Bartz, M.S. Akselrod, G. Denis, E.G. Yukihara,
242 Comparison between different readout approaches for aluminum oxide
243 radiophotoluminescent crystals, Radiation Measurements, 56 (2013) 361-364.

244 [19] J.M. Kalita, M.L. Chithambo, A comparative study of the dosimetric features of α -
245 Al₂O₃:C,Mg and α -Al₂O₃:C, Radiation Protection Dosimetry, 177 (2017) 261-271.

246 [20] J.M. Kalita, M.L. Chithambo, The influence of dose on the kinetic parameters and
247 dosimetric features of the main thermoluminescence glow peak in α -Al₂O₃:C,Mg,
248 Nuclear Instruments and Methods in Physics Research Section B: Beam Interactions with
249 Materials and Atoms, 394 (2017) 12-19.

250 [21] N.M. Trindade, L.G. Jacobsohn, Thermoluminescence and radioluminescence of α -
251 Al₂O₃:C,Mg at high temperatures, Journal of Luminescence, 204 (2018) 598-602.

252 [22] J.M. Kalita, M.L. Chithambo, The effect of annealing and beta irradiation on
253 thermoluminescence spectra of α -Al₂O₃:C,Mg, Journal of Luminescence, 196 (2018)
254 195-200.

255 [23] J.M. Kalita, M.L. Chithambo, Phototransferred thermoluminescence in α -
256 Al₂O₃:C,Mg under 470nm blue light stimulation, Journal of Luminescence, 188 (2017)
257 371-377.

258 [24] J.M. Kalita, M.L. Chithambo, G.S. Polymeris, Thermally-assisted optically
259 stimulated luminescence from deep electron traps in α -Al₂O₃:C,Mg, Nuclear Instruments
260 and Methods in Physics Research Section B: Beam Interactions with Materials and
261 Atoms, 403 (2017) 28-32.

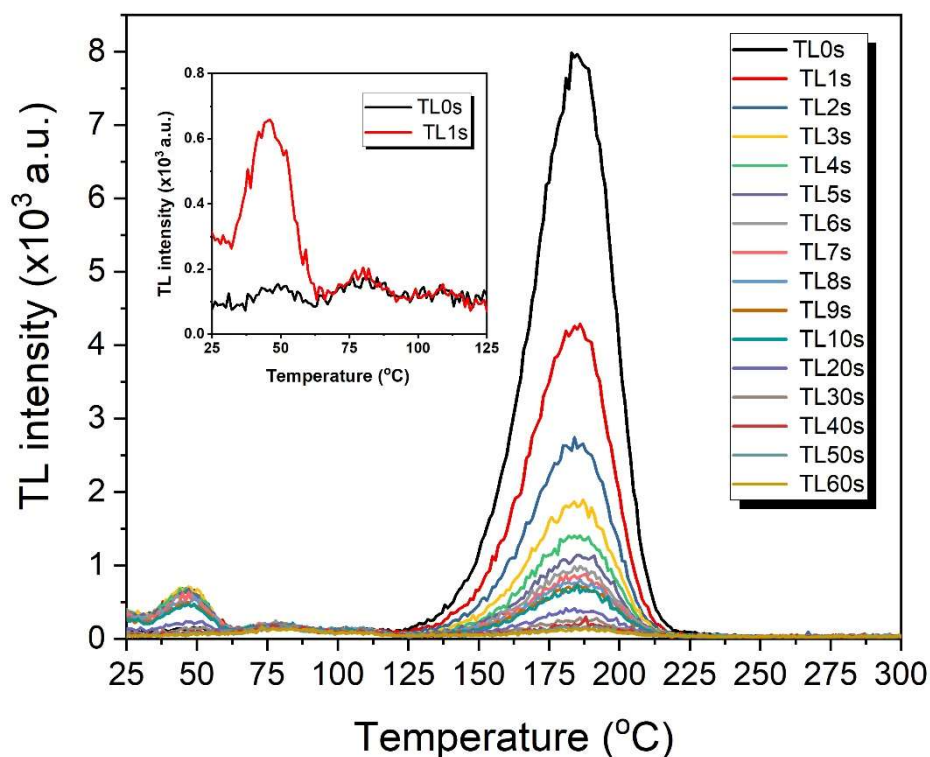
262

263

264 **FIGURE CAPTIONS**

265

266 **Figure 1** - TL glow curves of $\text{Al}_2\text{O}_3:\text{C},\text{Mg}$ single crystal obtained under different
267 illumination times using protocol A. The TL signal without previous illumination (TL0s)
268 time is included for comparison. The insertion shows the curve with highlight for the
269 sample without illumination and 1 second of illumination added. See text for details.



270

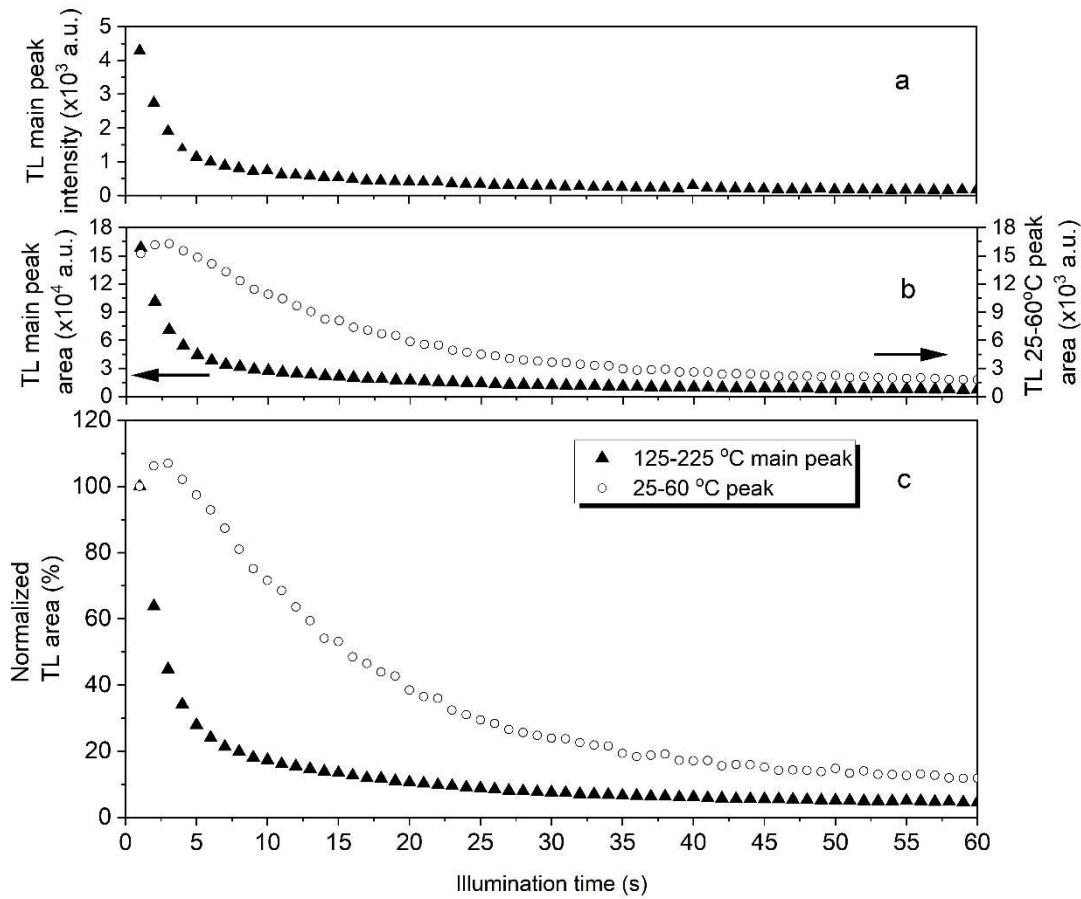
271

272

273

274

275 **Figure 2 - a)** Peak intensity value of the TL main peak (at 185 °C); **b)** area of the TL glow
 276 curve from RT to 60 °C (open circles), and of the main TL peak (125-225 °C; solid
 277 triangles); and **c)** TL area of the main TL peak (125-225 °C; solid triangles) and of the
 278 glow curve from RT to 60 °C (open circles) normalized to the respective area of the glow
 279 curve obtained with no illumination as a function of illumination time.



280

281

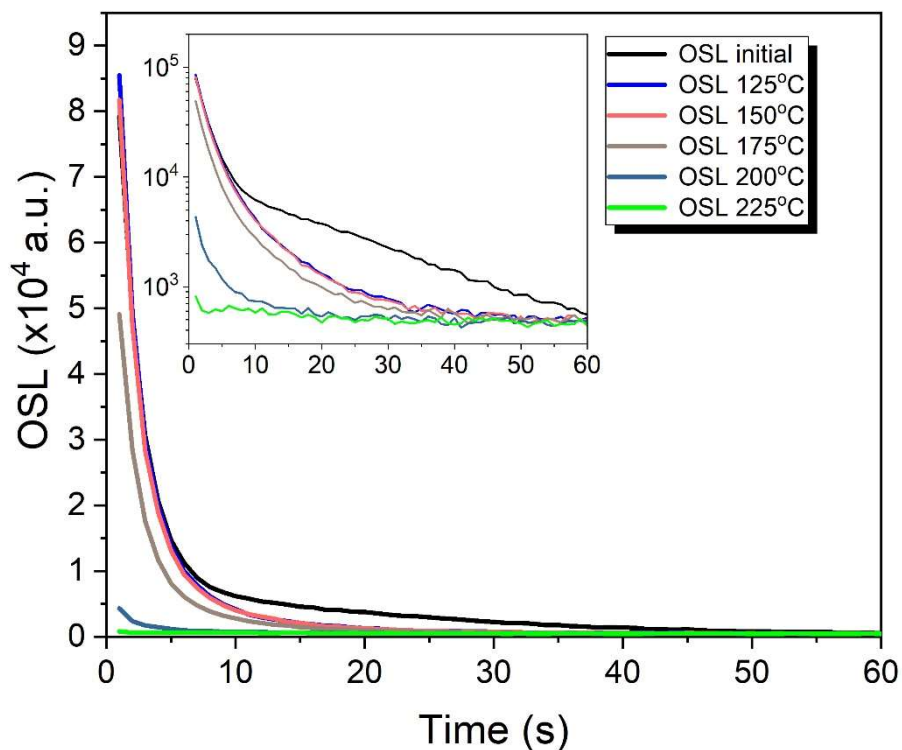
282

283

284

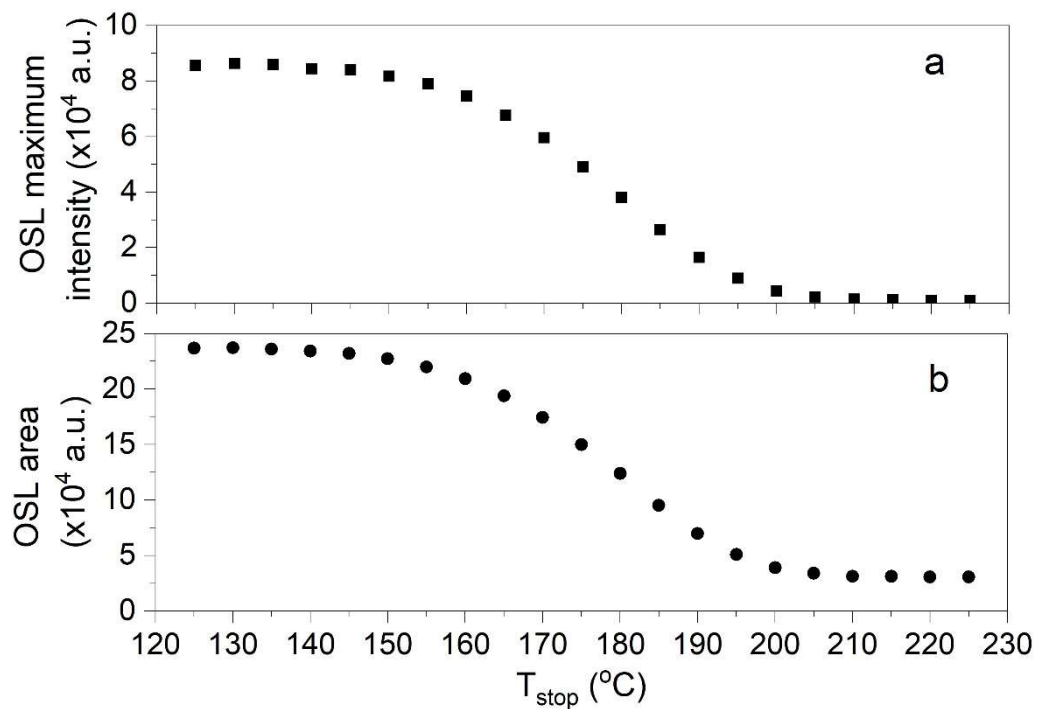
285

286 **Figure 3** - OSL signal of $\text{Al}_2\text{O}_3:\text{C},\text{Mg}$ single crystal obtained at room after heating till
287 selected temperatures (T_{stop}) using protocol B. The nomenclature OSL XXX °C
288 corresponds to the limit temperature at which the sample was heated before the
289 measurement at room temperature. The inset presents the same data in semi-log scale to
290 facilitate visual analysis. The OSL signal without previous thermal treatment (OSL
291 initial) is included for comparison. See text for details.



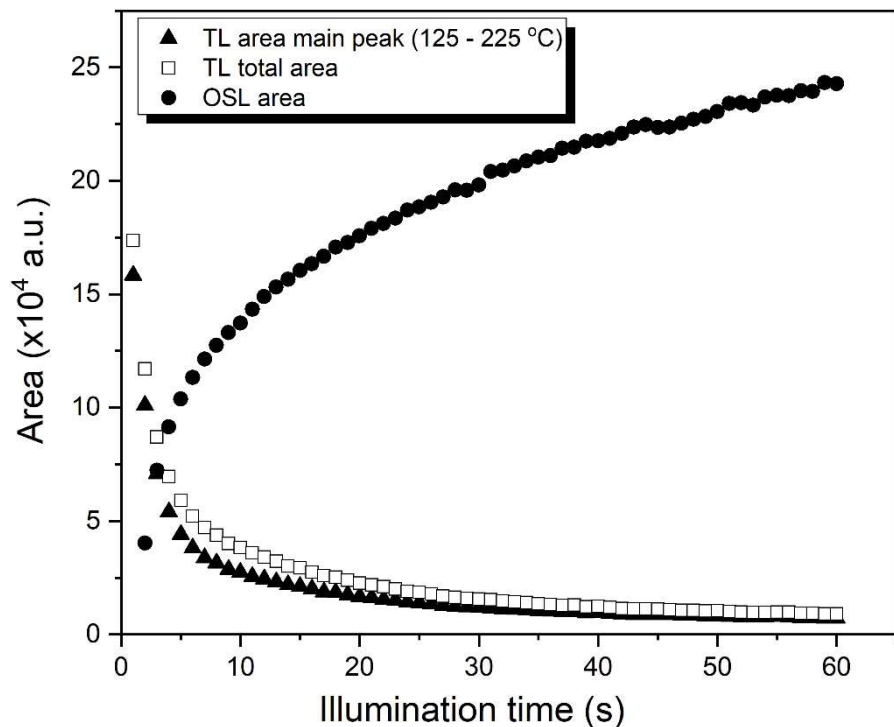
292
293
294
295
296
297

298 **Figure 4** – a) The OSL maximum intensity (*i.e.*, initial OSL signal value), and b) total
299 area under the OSL curve as a function of T_{stop} .



300
301
302
303
304
305
306
307
308
309
310

311 **Figure 5** – Integrated partial OSL signal (solid circles) and integrated TL signal after
312 OSL illumination (whole glow curve (open squares), and main peak (solid triangles)) as
313 a function of the illumination time.



314